McMASTER UNIVERSITY

HAMILTON, ONTARIO, CANADA

DEPARTMENT OF METALLURGY AND MATERIALS SCIENCE

DEVELOPMENT OF NON-LEADED FREE MACHINING STEELS-PHASE III

FINAL REPORT

April 1, 1983 - March 31, 1984

S.V. Subramanian

V. Meng and

D.A.R. Kay

Work on this project was conducted under the auspices of
Physical Metallurgy Research Laboratories
Canada Centre for Mineral and Energy Technology
Energy, Mines and Resources, Canada

DSS FILE NUMBER	:	13SV-23440-3-9134
DSS CONTRACT SERIAL NUMBER	:	OSV83-00048
CANMET PROJECT NUMBER	:	360251
CANMET SCIENTIFIC AUTHORITY	:	Mr. D.A. Parsons

August 1984

This report should be cited by D.S.S.
File No. 13SV-23440-3-9134

44 pp

MICROMEDIA

FEB 27 198

CONTENTS

		Page
	INTRODUCTION	1
1.	STEELMAKING	1
2.	MATERIALS CHARACTERISATION	3
	2.1 Chemical Analysis	3
	2.2 Microstructure	3
	2.3 Mechanical Properties	3
	2.4 Inclusion Characterisation	3
	2.4.1 Inclusion Analysis	3
	2.4.2 QTM Analysis	20
3.	MACHINABILITY ASSESSMENT	20
	3.1 Tool Geometry	23
	3.2 Cutting Conditions	23
	3.3 Test Results for Carbide Tools	24
	3.3.1 Flank Wear Tests	24
	3.3.2 Surface Finish	24
	3.3.3 Chip Form	24
	3.3.4 Cutting Forces	26
	3.4 Test Results for HSS Tools	26
	3.4.1 Flank Wear Tests	26
	3.4.2 Surface Finish	30
	3.4.3 Chip Form	30
	3.4.4 Cutting Forces	30
4.	DISCUSSION	32
	4.1 Machinability with Carbide Tools	32
	4.1.1 Flank Wear	32
	4.1.2 Cutting Forces	33
	4.2 Machinability with HSS Tools	33
	ACKNOWLEDGEMENTS	33
	REFERENCES	34
	APPENDIX	35

INTRODUCTION

Phase III of the project "Development of Non-Leaded Free Machining Steels", carried out in cooperation with Atlas Steels Co. Ltd. (Mr. L. Wigmore), the Department of Energy, Mines and Resources - CANMET (Dr. J.D. Boyd) and the Department of Mechanical Engineering, McMaster University (Dr. H. ElMaraghy), reports the results of the materials characterization and machinability assessment of five Atlas CM steel grades produced under specific deoxidation practices designed to control the composition and morphology of oxide and sulphide inclusions. The objective of the deoxidation programme was the elimination of the hard, abrasive alumina inclusions which adversely affect machinability in terms of tool wear, using niobium additions for the production of fine-grained steels when required.

Machinability assessment was carried out using both conventional and coated M2/M4 HSS tools, and coated carbide tools.

1. STEELMAKING (Atlas Steels Co. Ltd. - Mr. L. Wigmore)

The deoxidation practices and aim specifications of the four grades of Atlas CM grades produced, are summarized in Table I. Steel I is a standard practice Si-Al killed steel, designed to contain Al_2O_3 and MnS inclusions. Steel II is a Mn-Si deoxidized steel, with a Nb addition for grain refinement, designed to contain $MnO\text{-}SiO_2$ and MnS inclusions. Steel IV is a Ca-treated, Si-Al killed steel, designed to contain modified calcium aluminate/CaS and MnS inclusions. Two heats of Steel III, a Ca-Si treated steel with a Nb addition for grain refinement and designed to contain $CaO\text{-}Al_2O_3\text{-}SiO_2$ and MnS inclusions, were produced. Steel IIIA contained what appeared to be gehlenitic ($2CaO\text{-}Al_2O_3\text{-}SiO_2$) inclusions and Steel IIIB contained what appeared to be anorthitic ($CaO\text{-}Al_2O_3\text{-}2SiO_2$) inclusions.

TABLE I: Aim Specifications for Atlas CM Grades

DEOXIDATION PRACTICE	ATLAS CM (0.05/0.08%S)			
	I Standard Si - Al	II Mn - Si	III Si - Ca	IV Si-Al-Ca
AIM ANALYSIS Ca_{total}	<10	<10	30-100	>30
AIM ANALYSIS O_{total}	<30	>60	100	<30
AIM ANALYSIS Al_{total}	>160	<100	50 max	200 max
AIM ANALYSIS ppm Cb	---	350	350	---
OXIDE INCLUSIONS	Al_2O_3	MnO-SiO_2	CaO-Al_2O_3-SiO_2	CaO-Al_2O_3-CaS

Steel Grade	C	Mn	P	S	Si	Cr	Mo	Ni
ATLAS CM	0.37/0.42	0.90/1.20	0.040/max	0.05/0.08	0.15/0.30	0.25/max	0.05/0.12	0.40/max

2. MATERIALS CHARACTERIZATION

2.1 Chemical Analysis

The spectrochemical analyses of the five steels, as determined by Atlas and CANMET, are given in Table II. In general, the agreement between the two sets of analytical data is good. However, the Steel IV aluminum analyses do not agree well (0.047% vs. 0.020%) and the CANMET manganese and sulphur analyses are, on average, higher by 0.05% and 0.010%, respectively, for all steels. The Steel I silicon analyses again do not agree well (0.27% vs. 0.215%).

2.2 Microstructure (Ms. V. Meng, McMaster University)

The microstructure of all steels consisted of fine lamellar pearlite and well distributed ferrite. Representative micrographs are presented in Figures 1-5. Grain size estimates and hardness measurements are given below:

Steel	I	II	IIIA	IIIB	IV
ASTM Grain Size	8	7	8-9	7	7
Hardness (R_B)	91	89	92	93	91

2.3 Mechanical Properties (Atlas Steel Co. Ltd.)

Mechanical properties are listed in Table III. All steels were supplied by Atlas for machinability assessment and materials characterisation in the normalised condition (1-2 hours at 1575^{o}F and air-cooled).

2.4 Inclusion Characterisation (CANMET)

2.4.1 Inclusion Analysis (Mr. D. Parsons and Mrs. V. Moore)

Mid-radius longitudinal sections from each steel were examined metallographically, Figures 6-15, and the different inclusion types qualitatively

Table II: Spectrochemical Analysis - wt%*

Steel and Heat No.	Analysis	C	Mn	P	S	Si	Cr	Mo	Ni	Cu	Al	Sn	Pb	Ca	Nb
I H-1535	Atlas	.39	1.11	.016	.069	.29	.15	.05	.15	-	.04	.034	.002	-	-
	CANMET	.420	1.185	.015	.080	.215	.145	.050	.155	.155	.040	.020	-	-	<0.005
II J-1285	Atlas	.38	1.06	.018	.075	.16	.08	.06	.07	-	.003	.027	.002	-	.04
	CANMET	.410	1.145	.015	.085	.195	.085	.060	.070	.115	<.005	.010	-	-	.035
IIIA H-1904	Atlas	.36	1.19	.025	.065	.19	.20	.05	.13	.18	.003	.026	.003	-	.04
	CANMET	.370	1.235	.020	.075	.215	.200	.050	.125	.190	<.005	.025	-	-	.045
IIIB H-2225	Atlas	.39	1.15	.02	.067	.33	.17	.05	.13	-	.007	.02	.001	-	.06
	CANMET	.395	1.195	.020	.075	.325	.170	.050	.135	.205	<.005	.025	-	-	.060
IV H-2757	Atlas	.39	1.07	.023	.055	.29	.12	.05	.11	-	.047	.026	-	.0024	-
	CANMET	.400	1.100	.020	.065	.300	.115	.050	.115	.115	.020	.020	-	-	<.005

*Steels contain <0.005% Ti and V.

TABLE III - Mechanical Properties

STEEL	NORMALISED					
	Y.S psi	UTS psi	Elong %	R.A. %	BHN	CVN ft. lbs.
I	60200	97200	27	54.5	179/187	80/92/106
II	60500	93500	25	50	179	30/33/34
IIIA	67000	98500	25	55.5	187/192	98/108/134
IIIB	65000	104000	22	49.5	197/201	62/76/86
IV	60000	98500	25	51.5	187	47/48/49

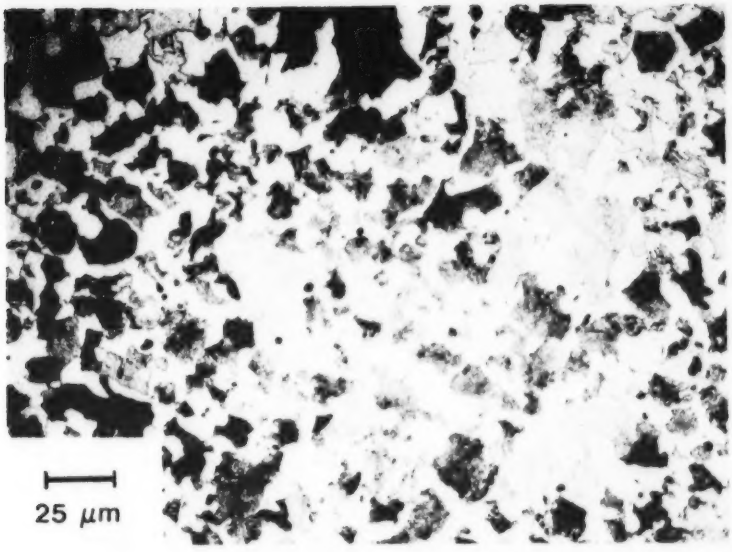

Figure 1: Steel I: Microstructure. Fine lamellar pearlite with good ferrite distribution. Etchant: 2% nital. Grain size: ASTM 8.

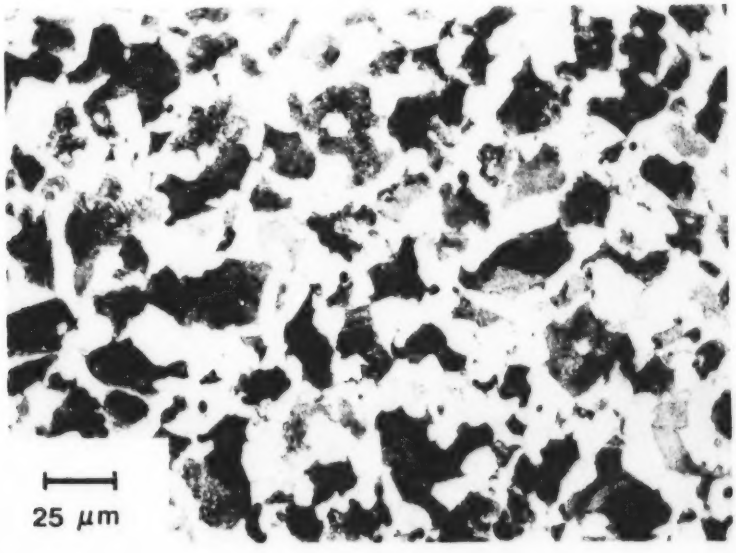

Figure 2: Steel II: Microstructure. Fine lamellar pearlite with good ferrite distribution. Etchant: 2% nital. Grain size: ASTM 7.

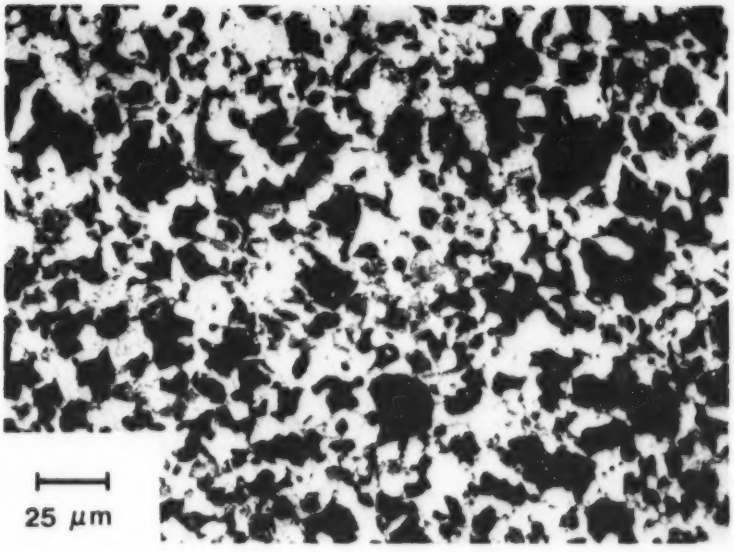

Figure 3: Steel IIIA: Microstructure. Fine lamellar pearlite with good ferrite distribution. Etchant: 2% nital. Grain Size: ASTM 8-9.

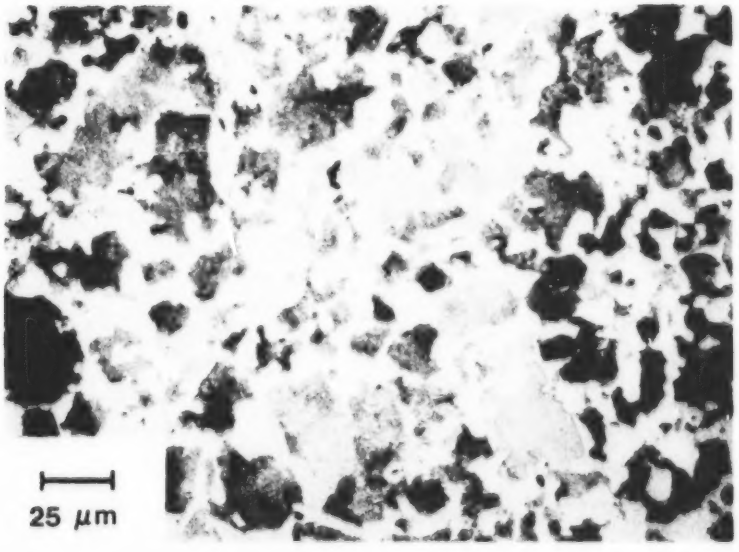

Figure 4: Steel IIIB: Microstructure. Fine lamellar pearlite with good ferrite distribution. Etchant: 2% nital. Grain size: ASTM 7.

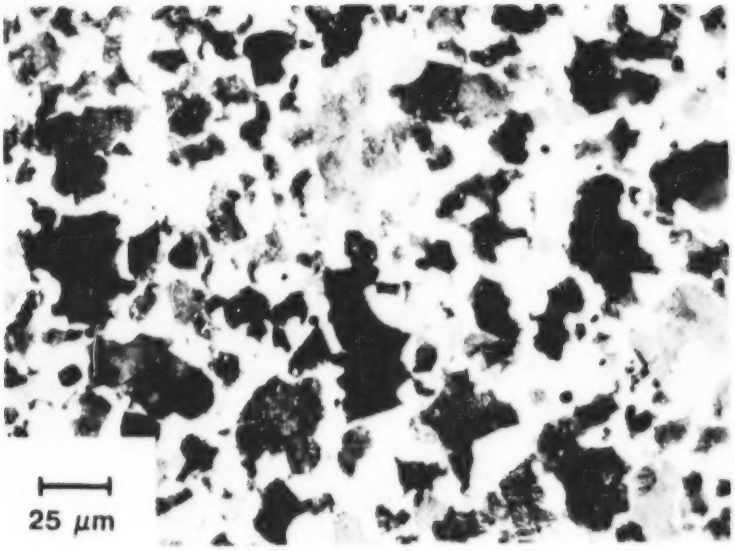

Figure 5: Steel IV: Microstructure. Fine lamellar pearlite with good ferrite distribution. Etchant: 2% nital. Grain size: ASTM 7.

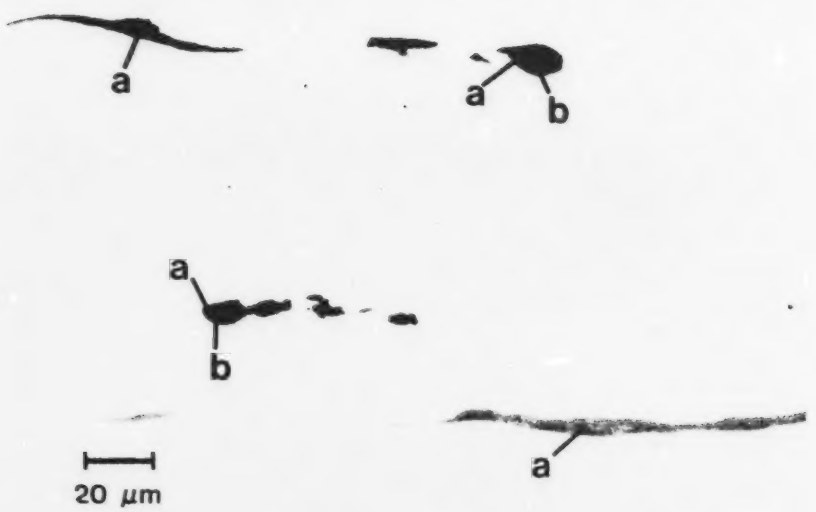

Figure 6: Steel I. Inclusion types: (a) MnS (b) Al_2O_3

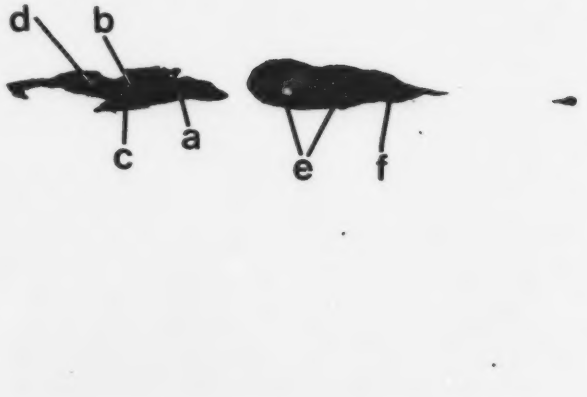

Figure 7: Steel II. Inclusion types: (a) manganese silicate (b) - (d) mullite/anorthite (inclusions II-7-b and II-7-d) (e) Al_2O_3/MnO/MgO (f) mullite/anorthite (inclusion II-7-f).

Refer to Tables A, B and C in the appendix for identification of inclusion numbers.

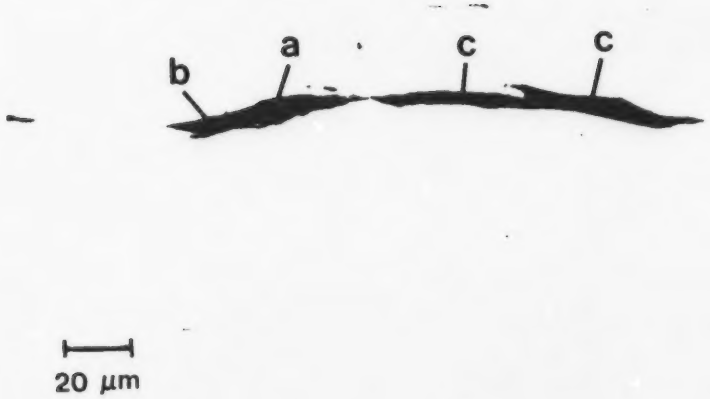

Figure 8: Steel II. Inclusion types: (a) mullite/anorthite (b) MnS (c) mullite/anorthite.

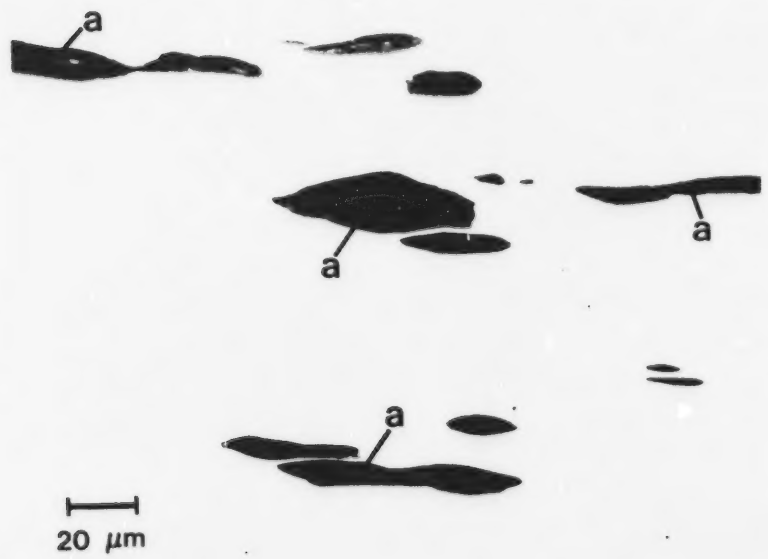

Figure 9: Steel II. Inclusion types: (a) MnS.

Refer to Tables A, B and C in the appendix for identification of inclusion numbers.

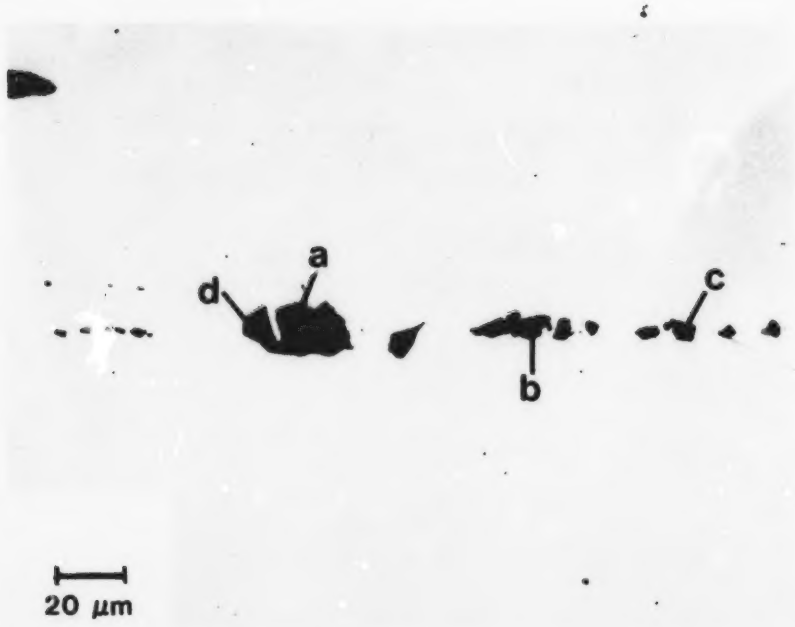

Figure 10: Steel IIIA. Inclusion types: (a) gehlenite (inclusion IIIA-10-a) (b) pseudo-wollastonite (inclusion IIIA-10-b) (c) pseudo-wollastonite (d) gehlenite.

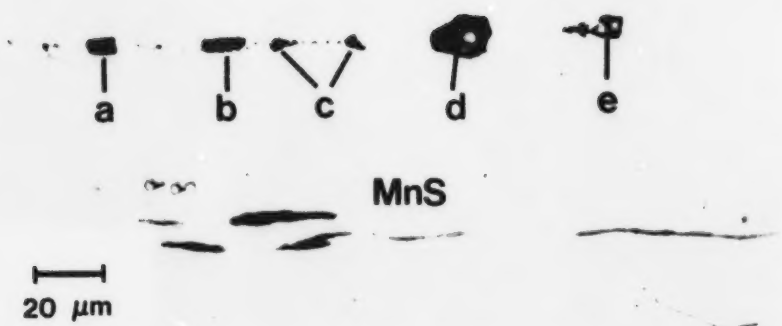

Figure 11: Steel IIIA. Inclusion types: (a) pseudo-wollastonite (inclusion IIIA-11-a); (b) MnS with pseudo-wollastonite tips; (c) pseudo-wollastonite (inclusion IIIA-11-c); (d) gehlenite(inclusion IIIA-11-d); (e) gehlenite.

Refer to Tables A, B and C in the appendix for identification of inclusion numbers.

Figure 12: Steel IIIB. Inclusion types: (a) gehlenite (inclusion IIIB-12-a) (b) crystalline Al_2O_3/MgO with traces of Mn (c) anorthite (inclusion IIIB-12-c) (d) anorthite (inclusion IIIB-12-d).

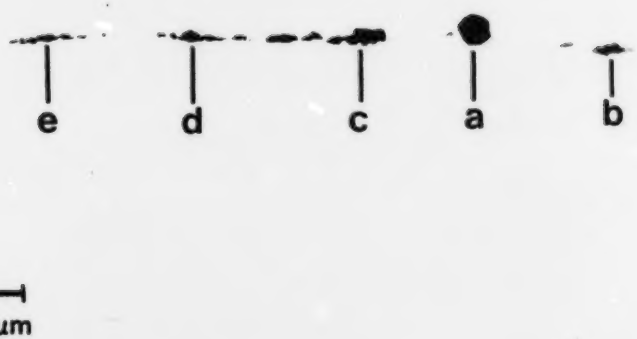

Figure 13: Steel IIIB. Inclusion types: (a) crystalline Al_2O_3/MgO with traces of Mn (b) MnS with anorthite edges (c) anorthite (inclusion IIIB-13-c) (d) MnS with anorthite edges (e) anorthite with trace of Mn (inclusion IIIB-13-e)

Refer to Tables A, B and C in the appendix for identification of inclusion numbers.

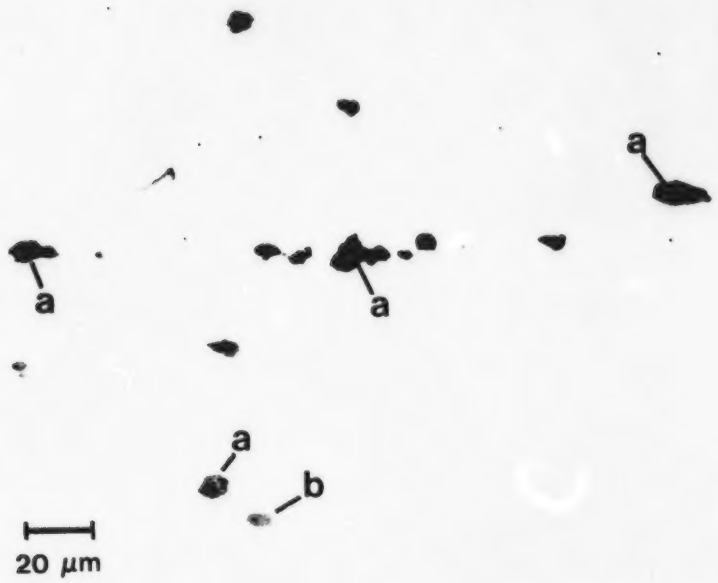

Figure 14: Steel IV: Inclusion type: (a) light area MnS/CaS; dark area Al_2O_3/MgO (b) MnS with trace of Ca.

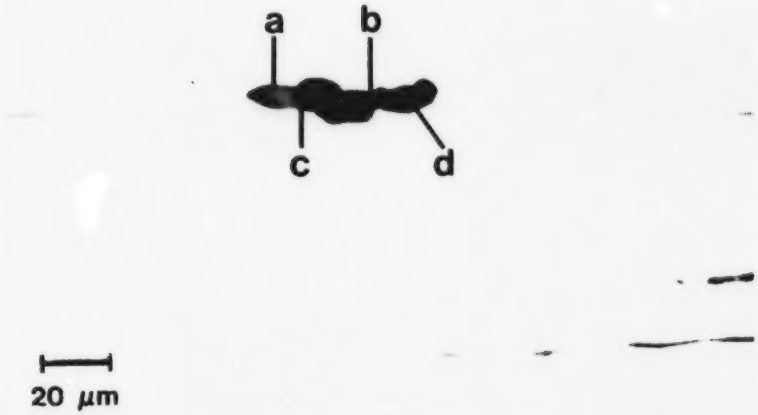

Figure 15: Steel IV: Inclusion type: (a) MnS with trace of Ca (b) MnS with trace of $CaO/Al_2O_3/SiO_2$ (c) Al_2O_3 with trace of CaS (d) MnS.

Refer to Tables A, B and C in the appendix for identification of inclusion numbers.

identified by microprobe analysis. Quantitative elemental microprobe analyses were carried out on selected inclusions in Steels II, IIIA, and IIIB, see Table A given in the Appendix. The alphanumeric inclusion identification in Table A is the same as that used in the captions of Figures 7, 10, 11, 12 and 13.

The elemental Ca, Al and Si contents of the oxide inclusions in Steels IIIA and IIIB, expressed in terms of the weight percent contents of their respective oxides - CaO, Al_2O_3 and SiO_2 - and normalized to 100%, are given in Table B in the Appendix. The inclusion type, also given in Table B, was determined by plotting the percentage oxide contents on a ternary $CaO-Al_2O_3-SiO_2$ phase equilibrium diagram, see Figures 16 and 17. The white areas on these $CaO-Al_2O_3-SiO_2$ phase diagrams represent the compositions of oxide inclusions which are "soft" relative to the matrix at high temperatures.

The elemental Ca, Mn, Al and Si analyses of the oxide inclusions in Steel II, expressed in terms of the weight percent contents of their respective oxides - CaO, MnO, Al_2O_3 and SiO_2, and normalized to 100% are also given in the Appendix, Table C. These inclusion compositions are plotted on the $CaO-Al_2O_3-SiO_2$ equilibrium phase diagram by making the approximation (CaO + MnO) ≡ MnO, Figure 18a, see Text. The white area in Figure 18b also represents the compositions of inclusions which are "soft" relative to the matrix at high temperatures. The approximate compositions shown in both Figures 18a and 18b indicate that "soft" oxide inclusions can be produced in Atlas CM grades by simple Mn-Si deoxidation. Complex inclusions of this type have been designated "Mullite/anorthite" in Table C.

A summary of the inclusion types found in each steel is given below:

Steel I

1. Elongated MnS inclusions, Figure 6.
2. Chubby MnS inclusions decorated with Al_2O_3, Figure 6.

Steel II

1. Fe(Nb) - NbC eutectic (not illustrated).
2. Large, chubby or elongated MnS inclusions (Figures 8 and 9).
3. Complex $CaO-MnO-Al_2O_3$ silicates (Figures 7 and 8).

Steel IIIA

1. Elongated MnS inclusions (Figure 11).
2. Small broken pseudowollastonitic-$CaO.SiO_2$-inclusions (Figures 10 and 11).
3. Large crystalline gehlenitic-$2CaO.Al_2O_3.SiO_2$ inclusions (Figures 10 and 11).
4. Fe(Nb) - NbC eutectic (not illustrated).

Steel IIIB

1. Short MnS inclusions (Figures 12 and 13).
2. Crystalline $MgO-Al_2O_3$ inclusions (Figures 12 and 13).
3. Large crystalline gehlenitic-$2CaO.Al_2O_3.SiO_2$ inclusions (Figures 12 and 13).
4. Small, thin anorthitic-$CaO.Al_2O_3.2SiO_2$-inclusions (Figures 12 and 13).

Steel IV

1. Elongated MnS inclusions (not illustrated).
2. MnS/CaS inclusions complexed with Al_2O_3/MgO (Figure 14).
3. MnS inclusion with trace of CaS or $CaO-Al_2O_3-SiO_2$ (Figures 14 and 15).
4. CaS with Al_2O_3 core (Figure 15).

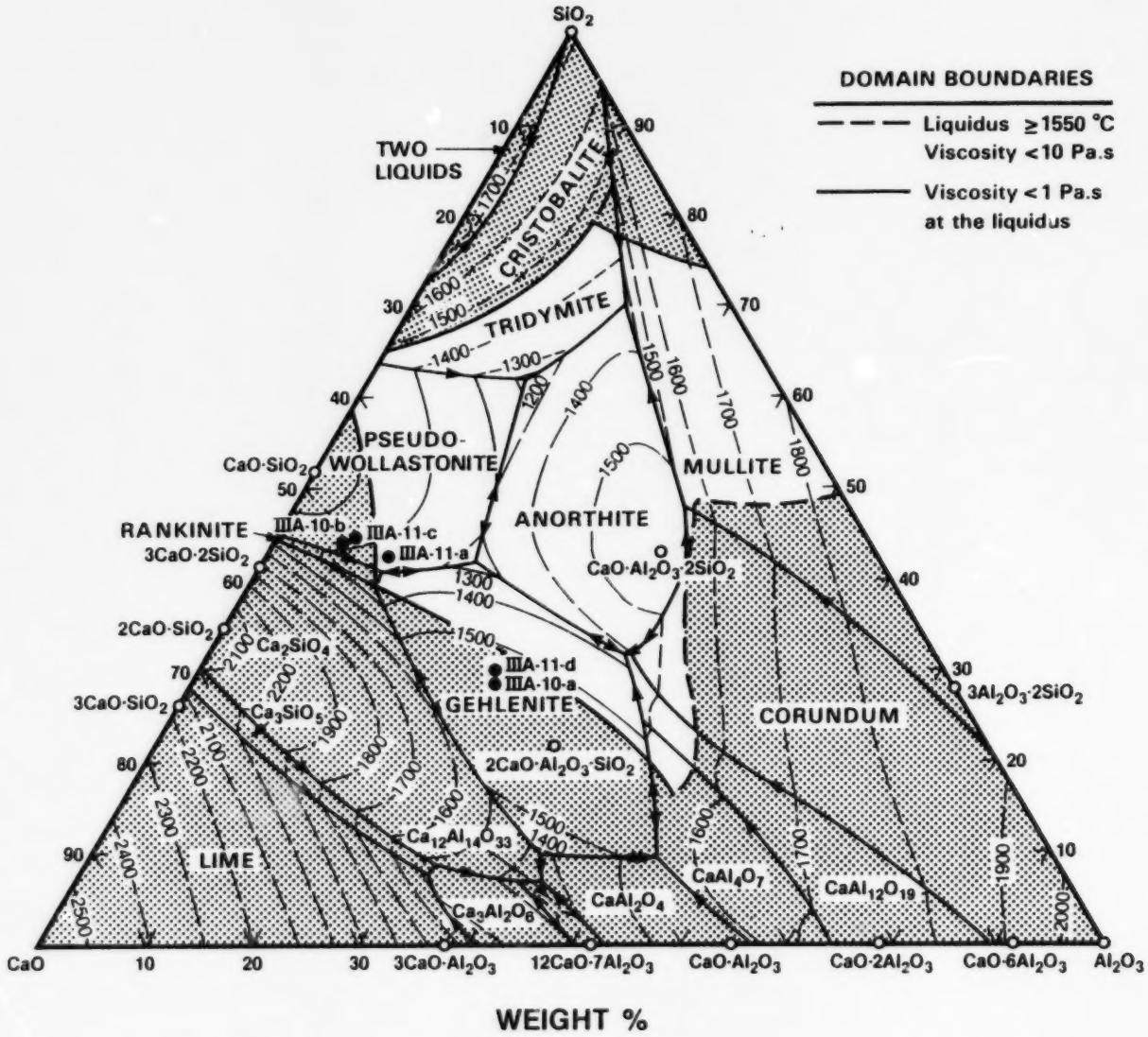

Figure 16: The CaO - Al_2O_3 - SiO_2 Phase Diagram giving Compositions of Inclusions in Steel IIIA (refer to Tables A and B in the Appendix).

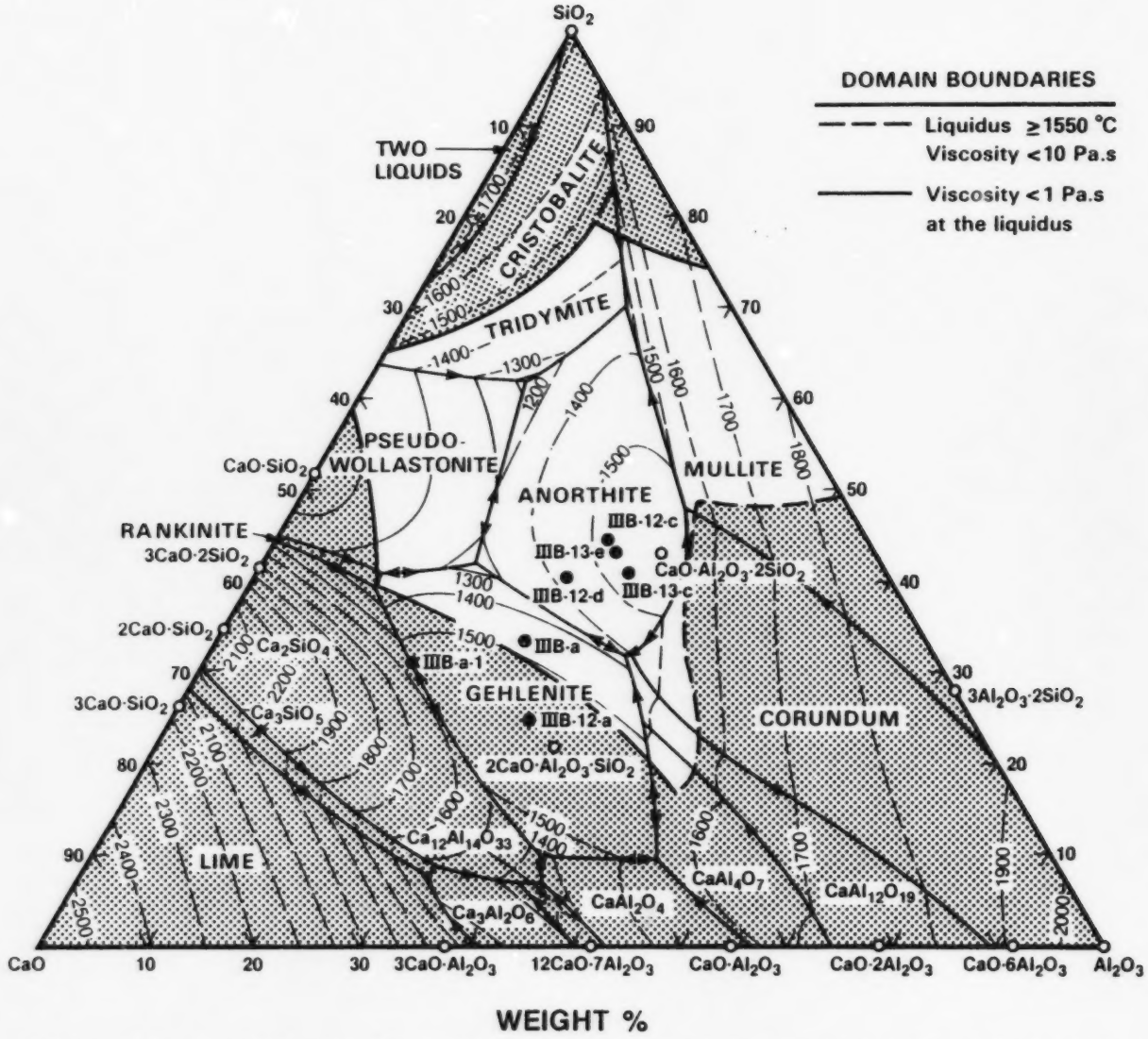

Figure 17: The CaO - Al_2O_3 - SiO_2 Phase Diagram giving Compositions of Inclusions in Steel IIIB (refer to Tables A and B in the Appendix).

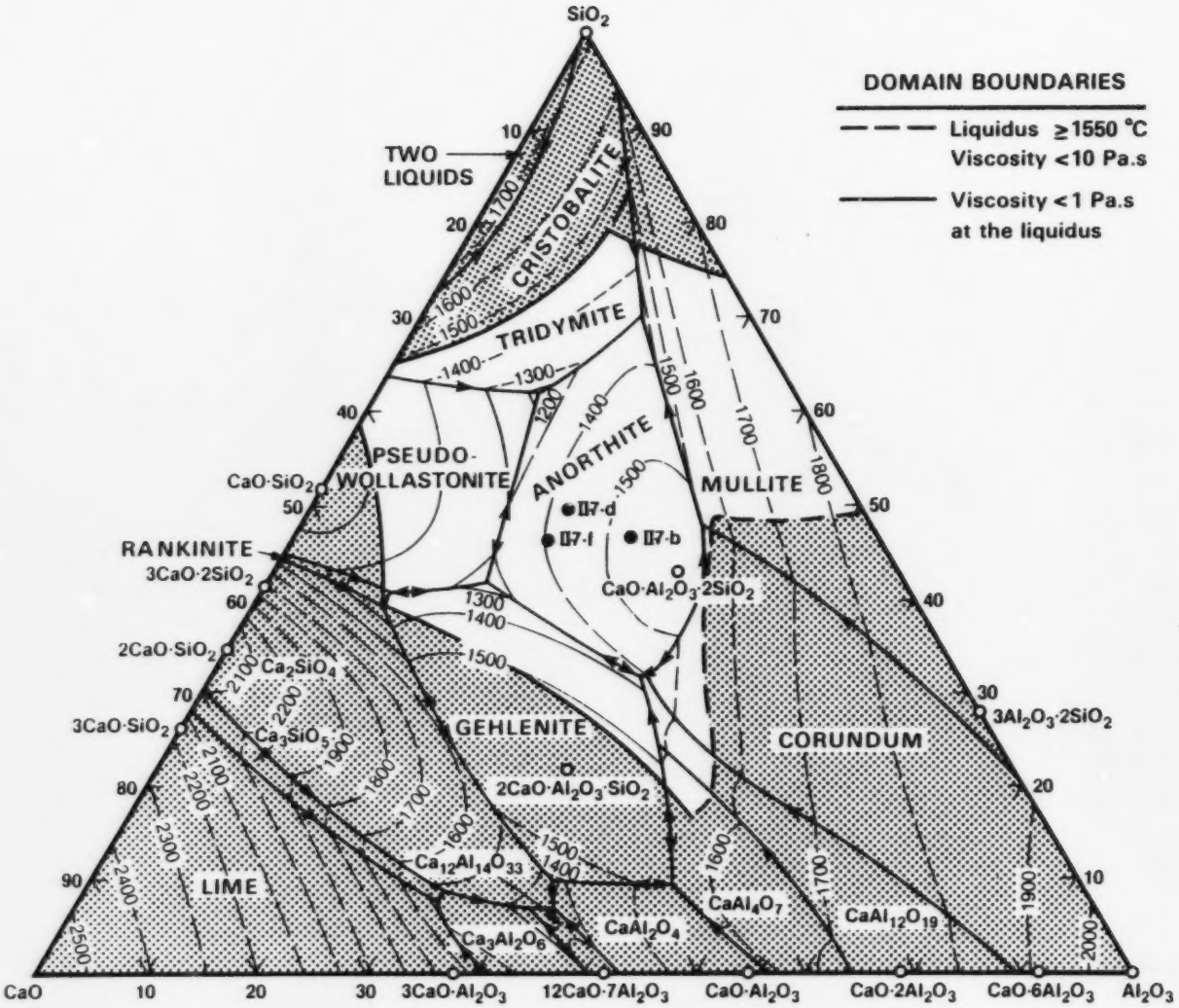

Figure 18(a): The CaO - Al_2O_3 - SiO_2 Phase Diagram giving Compositions of Inclusions in Steel II (refer to Tables A and C in the Appendix).

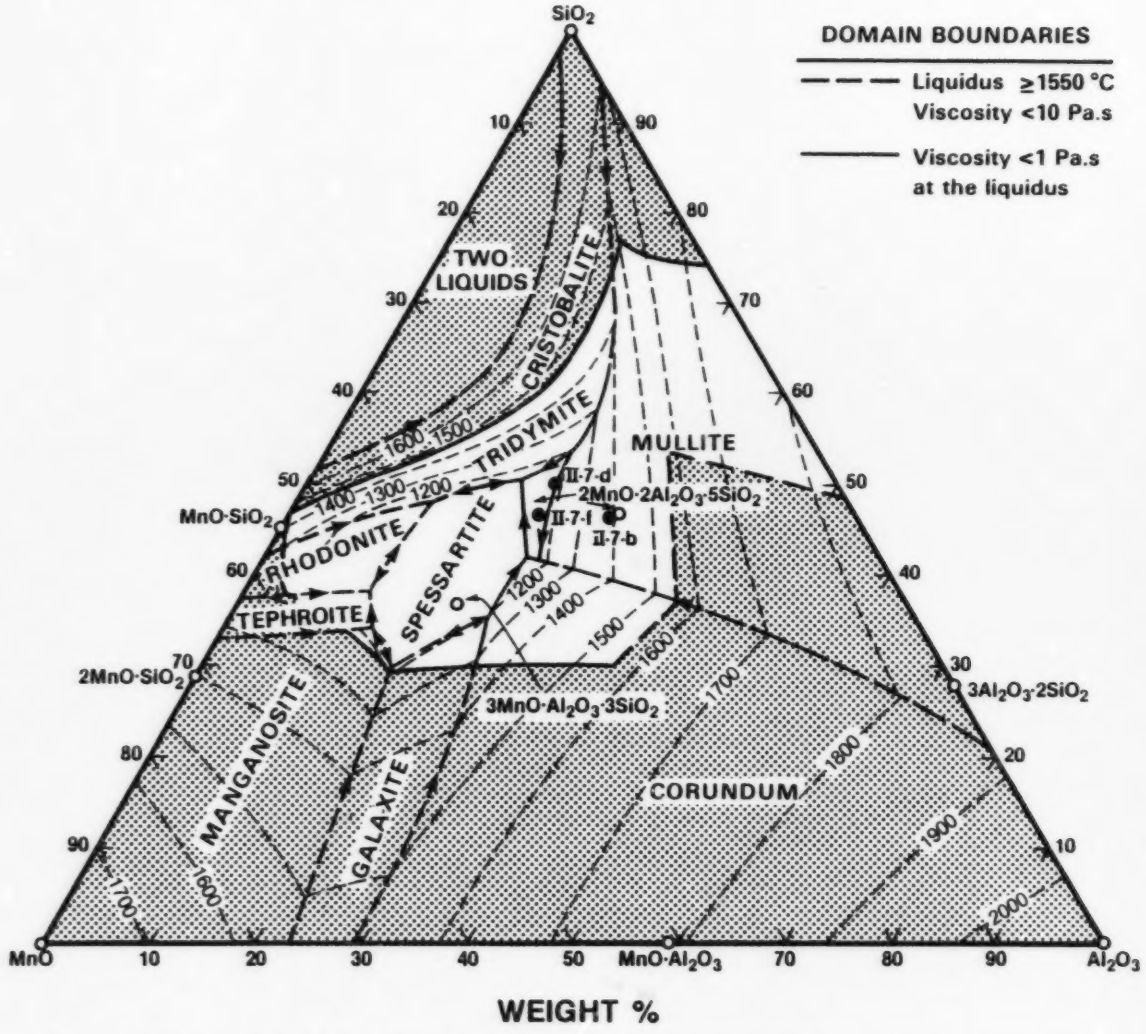

Figure 18(b): The MnO - Al_2O_3 - SiO_2 Phase Diagram giving Compositions of Inclusions in Steel II (refer to Tables A and C in the Appendix).

2.4.2 QTM Analysis (Dr. M. Shehata)

The results of the QTM analysis of the oxide and sulphide inclusions in the five steels, expressed in terms of their percentage by volume (vol. %), the number of inclusions per mm^2 (# mm^2) and their shape and size, are presented in Table IV. The size distributions of the oxide and sulphide inclusions, expressed as the number of inclusions per cm^2 (# cm^2), are given in Tables D and E, respectively, in the Appendix.

The oxygen and nitrogen contents of all five steels, as determined by the LECO TC-136 oxygen/nitrogen analyzer at McMaster, are presented in Table V together with the corresponding spectrochemical sulphur analyses taken from Table I. The correlation between the vol. % of oxide and sulphide inclusions given in Table IV and the bulk oxygen and sulphur analyses given in Table V is poor. This poor correlation may be due to difficulties in differentiating between oxides and sulphides by QTM analysis, in the complex oxide/sulphide inclusions found in these steels, or the presence of variable amounts of oxygen and sulphur in solution in the solid samples. Clearly, the QTM analysis and the spectrographic chemical analysis must be compatible before any rationalization of machinability in terms of oxide and sulphide distributions can be attempted.

3. MACHINABILITY ASSESSMENT (1) - (Dr. H. ElMaraghy and Dr. W. Zaton)

Single point turning machinability tests on the five Atlas CM grades were carried out on the MAZAK lathe of the Metal Cutting Laboratory at McMaster University (Dr. H. ElMaraghy and Dr. W. Zaton). Cutting tests were carried out using Sandvik 1025 TiC coated carbide inserts and two grades of high speed steel (HSS): the commonly used, conventional M2 grade and the high vanadium M4 grade. Sandvik Coromant TPMR432 triangular positive inserts, with a

Table IV: Quantitative Metallographic Results for Atlas Steels

STEEL	Oxide Inclusions > 2 μm					Sulphide Inclusions > 2 μm				
	vol.%	#/mm^2	Average Length μm	Average Breadth μm	Average Aspect Ratio	vol.%	#/mm^2	Average Length μm	Average Breadth μm	Average Aspect Ratio
*I	0.0228	4.8	5.86	4.58	1.37	0.367	168	8.76	3.18	2.42
II	0.0140	1.9	5.74	5.67	1.23	0.332	91	10.4	3.95	2.21
IIIA	0.0097	6.1	4.74	3.41	1.61	0.458	219	7.96	3.32	2.11
IIIB	0.0108	4.5	6.23	3.96	1.84	0.656	418	6.49	3.19	1.91
*IV	0.0380	9.1	5.40	4.82	1.18	0.294	140	8.01	3.38	2.13

Vol.%: volume % of inclusions ≡ area % of inclusions

#/mm^2: number of inclusions/mm^2

Shape: the average aspect ratio of individual inclusions is not the ratio between average length and average breadth of all inclusions.

*Oxide and sulfide inclusions cannot clearly be distinguished by QTM analysis in these steels.

Table V: Oxygen, Sulphur and Nitrogen Analysis - ppm

Steel	Oxygen	Sulphur	Nitrogen
I	24/37	690/800	81/135
II	34/49	750/850	91/168
IIIA	59/60	650/750	155/165
IIIB	39/52	670/750	114/164
IV	26/39	550/650	69/84

Kennametal CBT-16F chipbreaker and KTGPR-1641D tool holder, were used.

3.1 Tool Geometry

The basic tool geometry is given below.

Tool	Carbide	HSS
Rake angle (α)	5^{o}	10^{o}
Relief angle (γ)	6^{o}	7^{o}
Side cutting edge angle	0^{o}	0^{o}

Steel IIIA was also cut with M2 and M4 HSS tools with a 14^{o} rake angle. The carbide inserts had integral double chip-breaking grooves formed on their faces. There were no chip forming grooves on the HSS tools.

3.2 Cutting Conditions

The following cutting conditions were used.

Tool	Carbide	HSS
Cutting speed (V)	180 m/min	30, 45 and 60 m/min
Feed rate (f)	0.10 and 0.175 mm/rev	0.10 mm/rev
Depth of cut (b)	2 mm	2 mm

No cutting fluid was used.

3.3 Test Results for Carbide Tools

3.3.1 Flank Wear Tests

Initial tests at a feed rate of 0.1 mm/rev and a cutting speed of 180 m/min. gave little tool wear in tests of 30 minutes duration and despite the presence of the formed chip breaker, ribbon-type chips which tended to tangle around the workpiece were formed. The duration of the test was extended to 80 minutes and the feed rate increased to 0.175 mm/rev. in order to obtain short, slightly curled chips. Cutting was interrupted at 10 minute intervals and the flank wear measured.

The flank wear results are presented in Figure 19 as a function of cutting time at a cutting speed of 180 m/min. Steel I caused the highest tool wear due to the presence of the highly abrasive alumina inclusions, Figure 6, and at the end of the test the TiC layer was stripped off the cutting edge. The remainder of the steels performed similarly and although the flank wear was clearly visible, the TiC layer was not removed from the flank. Even at the end of these tests the inserts maintained their perfect cutability.

3.3.2 Surface Finish

There was no significant difference between the five steels tested and the surface finish after machining was excellent. In the case of Steel I, tiny sharp marks were scattered on the surface.

3.3.3 Chip Form

As mentioned above, the chip was curled and broken into short pieces at a feed rate of 0.175 mm/rev. For Steel I and Steel IV, the chipbreaker shim had to be minimally adjusted to obtain short chips. Longer, helical ships were sometimes

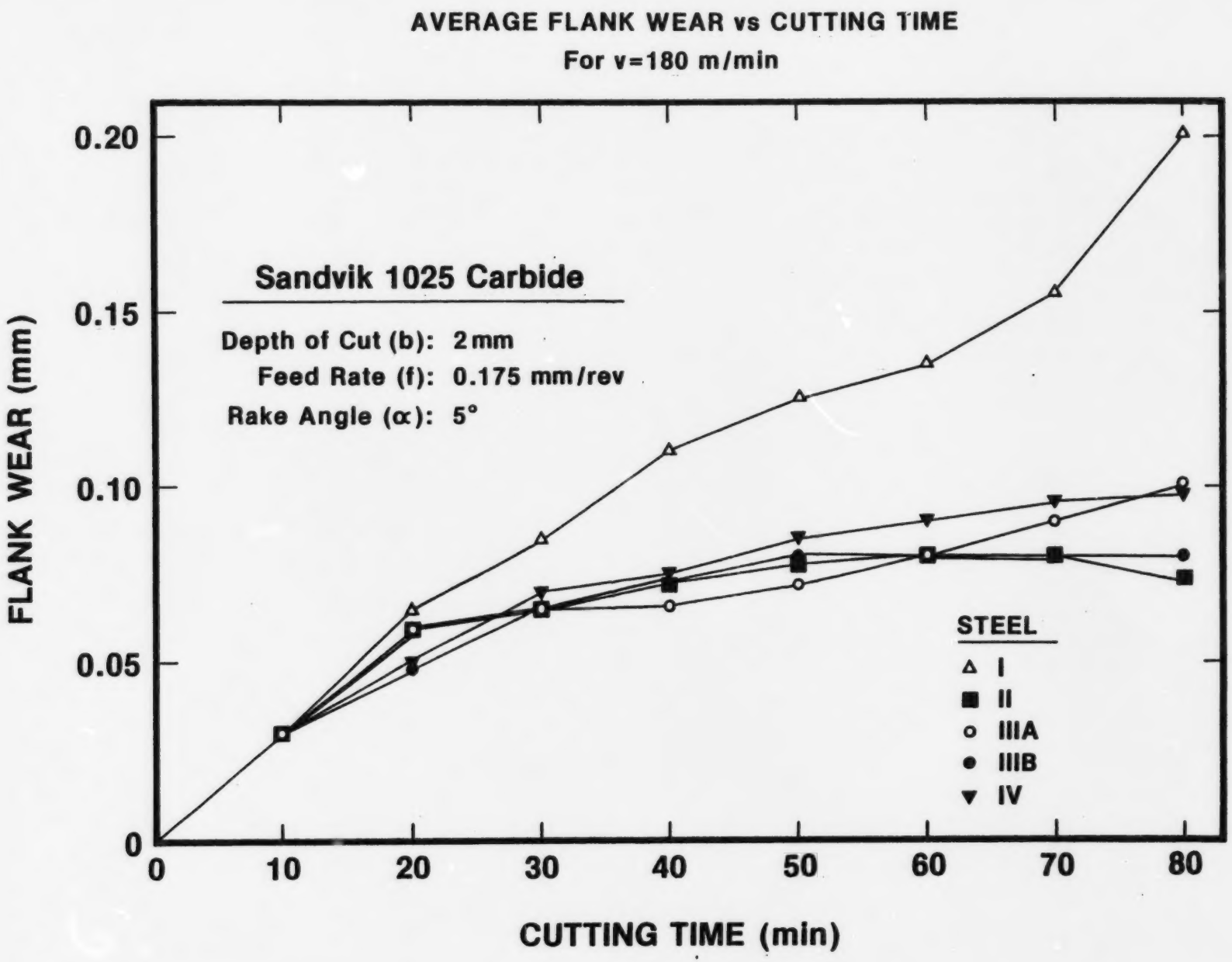

Figure 19: Average Flank Wear versus Cutting Time for v = 180 m/min. Sandvik 1025 Carbide

observed for partly worn inserts.

3.3.4 Cutting Forces

In separate tests, the tangential and feed components of the cutting force, F_T and F_N respectively (see Appendix, Figure A1), were measured and the results are presented in Figure 20. There is no substantial difference between the different steel grades although Steel II exhibits the lowest measured values for both force components.

3.4 Test Results for HSS Tools

3.4.1 Flank Wear Tests

Flank wear tests were carried out for both M2 and M4 type HSS tools for up to 60 minutes duration at cutting speeds of 30, 45 and 60 m/min. with a depth of cut of 2 mm and a feed rate of 0.1 mm/rev. Initial tests at a cutting speed of 90 m/min. resulted in the almost instantaneous thermal failure of the tool.

A stable built-up edge (BUE) formed on both types of tool at all cutting speeds and adhered strongly to the tool face. This BUE assumed the role of the cutting edge, protecting the tool from wear, and as a result the 0.1 - 0.3 mm flank wear which occurred at the beginning of each test did not change substantially during cutting.

The test results are presented in Table VI and Figure 21. In Table VI, the upper number in each box corresponds to the flank wear, in mm, at the end of each test while the lower number, where given, represents the time in minutes at which the tool failed thermally. The absence of a lower number indicates that the test lasted 30 minutes.

The results of tool wear measurement are rather inconclusive but it can be

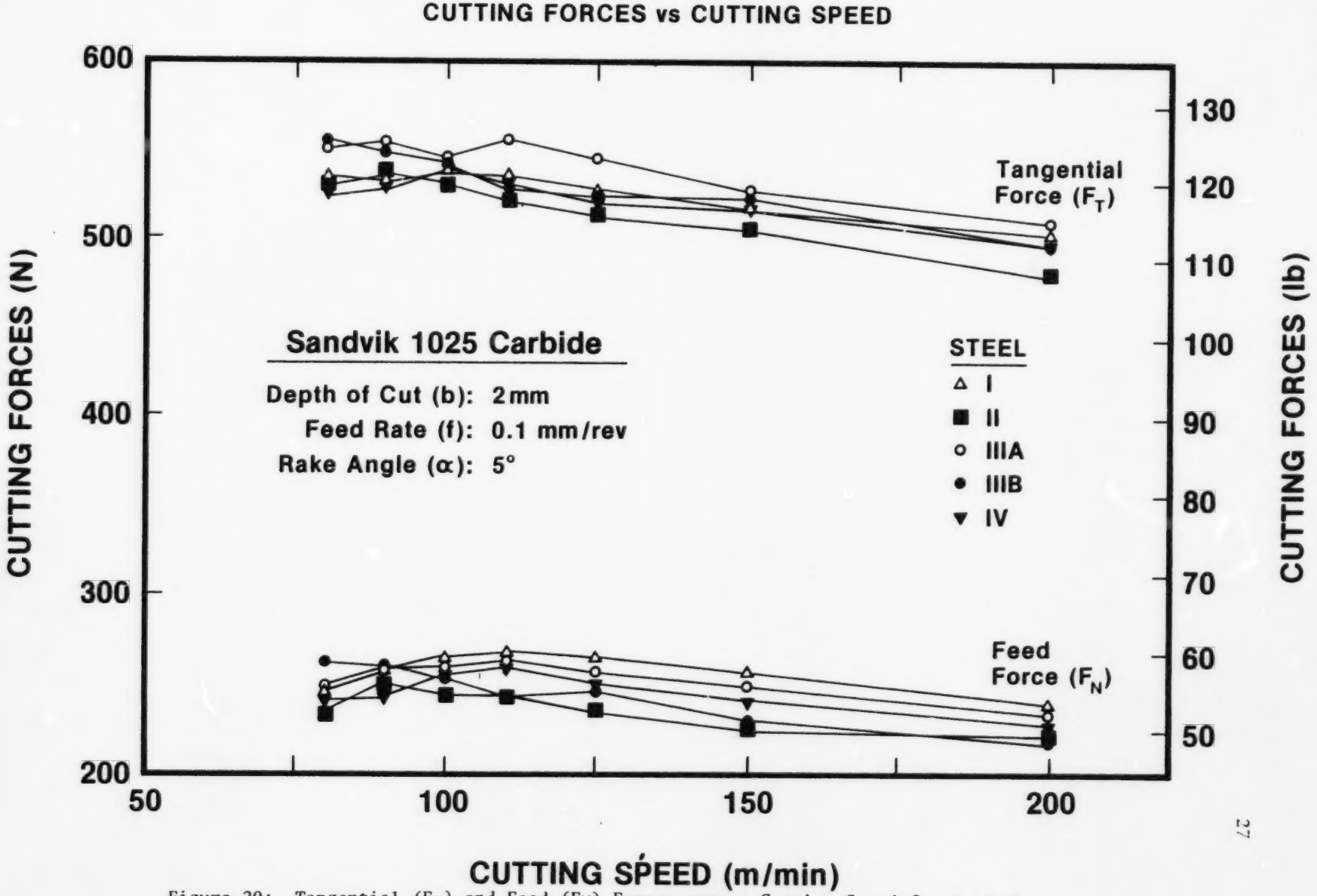

Figure 20: Tangential (F_T) and Feed (F_N) Forces versus Cutting Speed for Sandvik 1025 Carbide.

Table VI: HSS Tool Flank Wear Tests

HSS-type	M2			M4		
v(m/min) / Steel	30	45	60	30	45	60
I	.15	.28	.28	.20	.27	1 min
II	.15	.15	.27	.21	.23	.40 16 min
IIIA $\alpha = 14^{o}$	.16		.16 25 min	.19		.21
IIIA	.26	.22	.27 16 min	.20		.13 29 min
IIIB	.22		30 sec	.19	.15	30 sec
IV	.14	.22	.26 28 min	.23	.20	40 sec

Depth of cut (b): 2 mm Feed rate (f): 0.1 mm/rev.

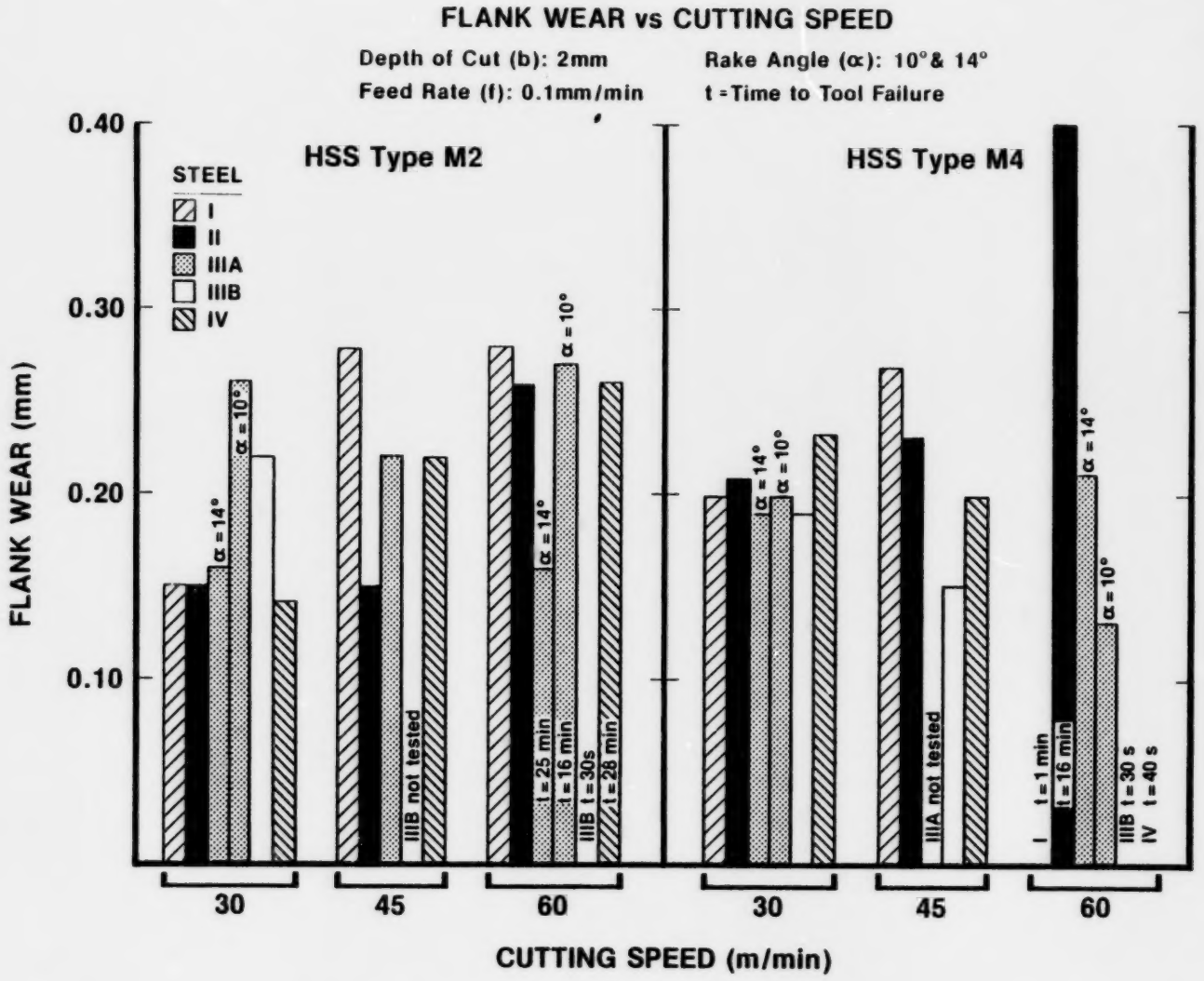

Figure 21: Flank Wear versus Cutting Speed for HSS Types M2 and M4.
Duration of Test: 30 min.

concluded that Steels II and IIIA exhibit the best performance in general. The increase in rake angle from 10 to 14 has a beneficial effect as far as the duration of the cut is concerned.

3.4.2 Surface Finish

The formation of a BUE resulted in a poor surface finish especially at a cutting speed of 30 m/min. The surface was matt, rough and covered with small particles of BUE. Better surface finishes were obtained at a cutting speed of 60 m/min. and by increasing the rake angle from 10 to 14^{o}.

3.4.3 Chip Form

Chip form did not vary significantly for the five grades tested. All chips were short and formed spirals with diameters up to 10 mm. At the beginning of cuts at speeds of 60 m/min., the chips were long with little curl, but after 1-2 minutes for M2 type HSS and 2-4 minutes for M4 type HSS the chips were short and arc type. This indicates that the crater formed on the face of the tool acted as a chip-curling groove. Only Steel IIIA gave spiral chips at cutting speeds of 60 m/min.

3.4.4 Cutting Forces

In separate tests, the tangential and feed components of the cutting force, F_T and F_N respectively (see Appendix, Figure A1), were measured and the results are presented in Figure 22. Both components have the lowest value in the cutting speed range 30-60 m/min. where the rather high BUE formed changes the tool geometry by increasing the effective rake angle, thus reducing the cutting force. As in the case of cutting with carbide tools, Steel II gave the lowest cutting force

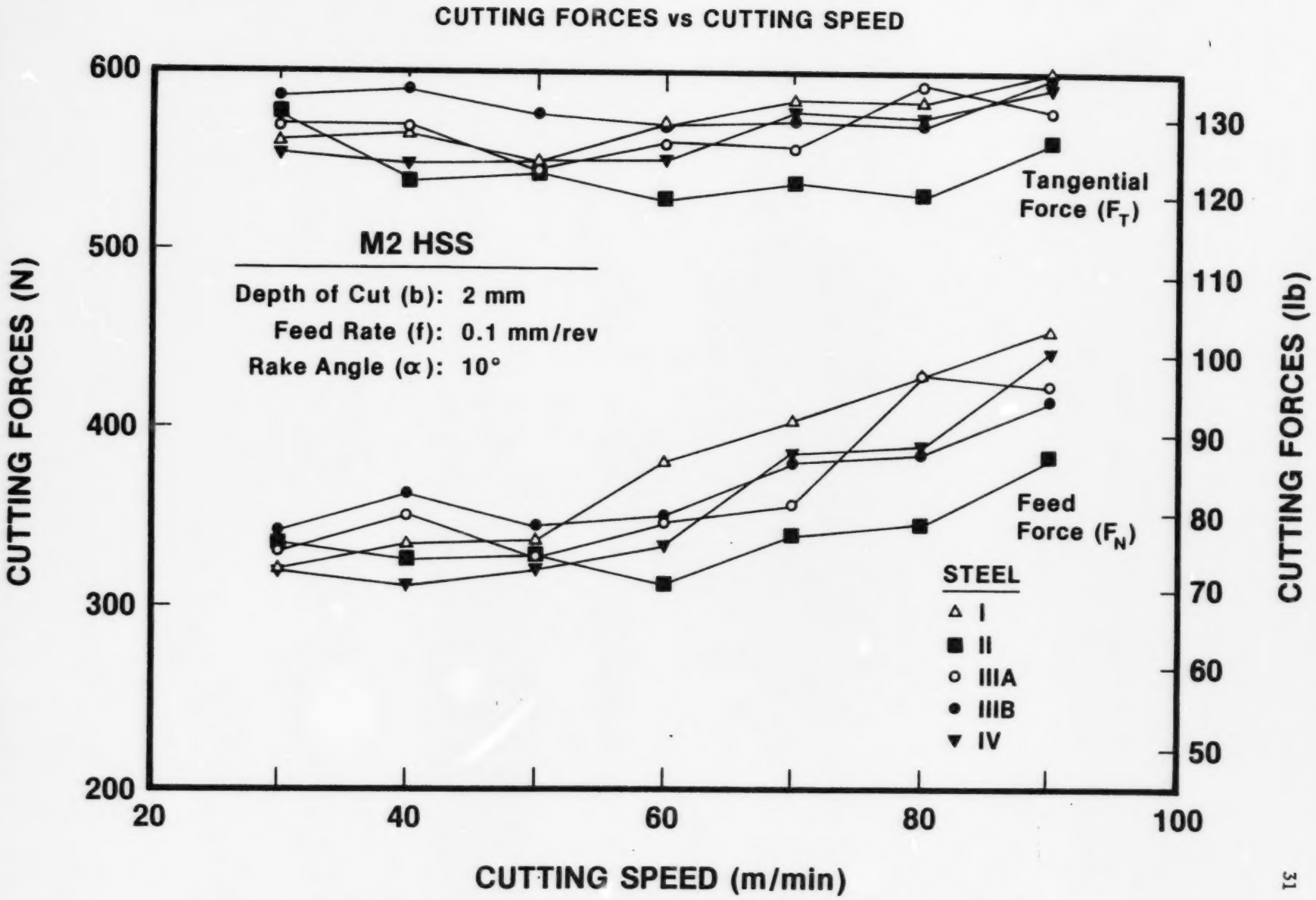

Figure 22: Tangential (F_T) and Feed (F_N) Forces versus Cutting Speed for M2 HSS.

and Steel I had the highest feed component at cutting speeds greater than 50 m/min.

4. DISCUSSION

4.1 Machinability with Carbide Tools

4.1.1 Flank Wear

Flank wear is primarily determined by the type of oxide inclusions present in the steel to be machined, i.e., whether they are 'hard' or 'soft' relative to the matrix at machining temperatures.

Steel I, produced by a standard Si-Al deoxidation practice, contained hard, abrasive Al_2O_3 inclusions complexed with MnS, and caused the most tool wear, Fig. 19. The other four steels caused less tool wear and performed similarly, Steel II performing marginally better than the other three. The Mn-Si deoxidation practice of Steel II, produced deformable $CaO-MnO-Al_2O_3-SiO_2$ inclusions, see Figures 8, 18a and 18b, which caused flank wear comparable to that produced by inclusions modified by calcium treatment.

None of the inclusion populations produced by Ca treatment were ideal with respect to the reduction of tool wear. Steel IIIA contained pseudowollastonitic/gehlenitic inclusions and Steel IIIB anorthitic/gehlenitic inclusions. The pseudowollastonitic and gehlenitic inclusions are crystalline in nature, Figures 10, 11 and 12, and are not as deformable as the anorthitic inclusions, Figures 12 and 13. The individual inclusion compositions, Figures 16 and 17, are quite far removed from the compositions of the low-melting ternary eutectics.

In Steel IV there is modification of alumina to the calcium aluminates by the Ca treatment, and the oxide inclusions are complexed with CaS and MnS, Figures

14 and 15.

4.1.2 Cutting Forces

There is no substantial difference between the measured cutting forces for the five steels, although Steel II shows the lowest value of both components, Figure 20. Cutting forces are primarily a function of the properties of the matrix and the lower values of the cutting force components may be attributed to the slightly lower yield stress for Steel II, Table III.

4.2 Machinability with HSS Tools

Cutting tests with both M2 and M4 type HSS tools were characterised by the formation of a very stable built-up edge (BUE). As a result, tool wear tests were inconclusive, Table VI and Figure 21, force components were rather high, Figure 22, and the surface finish was poor.

Preliminary cutting tests on Steels II and IIIA using TiN-coated M2 and M4 HSS tools gave greatly improved results. These tools showed a flank wear of about 0.1 mm after a cutting time of one hour, BUE formation was greatly reduced and the surface finish improved. The values of both cutting force components were also greatly reduced.

Work is continuing in this area.

ACKNOWLEDGEMENTS

The authors should like to acknowledge the financial support of the Department of Energy, Mines and Resources (CANMET). Materials characterisation was carried out by CANMET and the work of Dr. J.D. Boyd, Mr. D.A. Parsons, Dr. M. Shehata and Mrs. Vera Moore is gratefully acknowledged.

Machinability tests were carried out in the Department of Mechanical Engineering of McMaster University and the work of Dr. H. ElMaraghy and Dr. W. Zaton is gratefully acknowledged. The authors would also like to acknowledge the cooperation of Mr. Larry Wigmore of Atlas Steels Co. Ltd., in the production of the steels which are the basis of this report.

REFERENCES

1. W. Zaton and H. ElMaraghy: 'Machinability Tests of Five Atlas CM Steel Grades'. Department of Mechanical Engineering, McMaster University, July, 1984.

APPENDIX

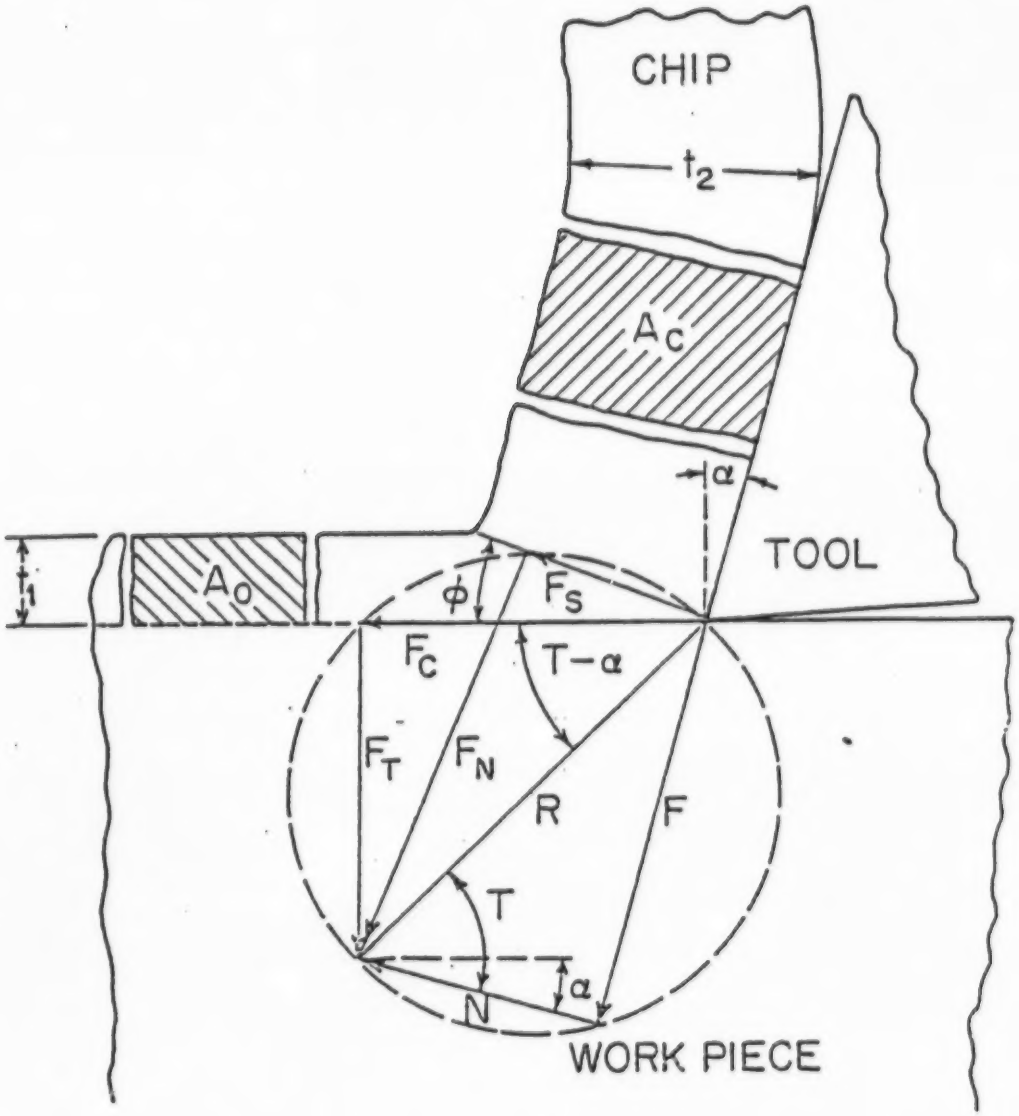

F_T in the text — F_C on this diagram

F_N in the text — F_T on this diagram

Figure A1: - The Composite Force Diagram of Merchant *

* Merchant, M.E., J. App. Phys., vol. 16, No. 5, 1945, pp. 267-75.

Table A. Elemental Microprobe Inclusions Analysis - wt%

Inclusions	Al	Si	Mg	S	Ca	Mn	Fe	Ti	0^{+}
II-7-b	13.73	18.48	0.37	0.17	9.24	5.06	4.87	0.54	47.54
*II-7-d	9.42	17.92	0.45	0.29	6.42	9.22	10.41	0.62	45.24
*II-7-f	10.01	17.97	1.76	0.21	5.75	13.29	1.37	2.27	47.38
IIIA-10-a	14.89 13.82	12.30 13.30	0.92 0.97	0.0 0.02	29.36 29.11	0.20 0.20	1.38 1.38	0.11 0.11	40.82 41.19
IIIA-10-b	2.73	16.91	0.0	0.72	28.54	1.11	5.44	2.64	41.92
IIIA-11-a	5.06	16.44	0.06	0.04	27.19	0.55	5.50	1.02	44.13
*IIIA-11-c	2.28 3.102	14.76 12.75	0.0 0.0	0.10 0.08	24.04 21.59	0.52 0.58	15.22 15.22	0.55 0.55	42.53 46.13
IIIA-11-d	13.43 13.99	13.48 13.00	1.27 1.04	0.01 0.01	28.82 29.10	0.34 0.29	1.45 1.45	0.01 0.01	41.18 41.10
IIIB-12-a	17.04 16.38	10.63 11.09	0.0 0.05	0.0 0.03	28.01 27.62	0.19 0.30	1.66 1.66	0.0 0.0	42.47 42.86
*IIIB-12-c	9.62	11.60	0.32	0.39	9.65	0.56	37.84	0.21	29.80
*IIIB-12-d	8.85	10.45	0.51	0.37	12.11	1.48	12.71	0.58	52.95
*IIIB-13-c	13.21	13.73	0.11	0.01	12.32	0.28	18.50	0.66	41.18
*IIIB-13-e	8.63	9.89	0.0	0.0	8.34	0.41	36.55	0.53	35.52
*IIIB-a	12.44	11.99	0.43	0.14	21.59	0.54	12.85	0.19	39.83
*IIIB-a-1	5.93	8.48	0.17	1.97	11.87	4.44	26.80	0.26	40.08

*Indicates precipitates are small or thin and most of Fe content is due to contribution from surrounding matrix.

+Oxygen calculated by difference.

Table B: Oxide Inclusion Composition - wt%

Inclusion	CaO = % Ca x 1.4	SiO_2 = % Si x 2.14	Al_2O_3 = % Al x 1.89	(CaO + SiO_2 + Al_2O_3) ≡ 100			Type
				CaO	SiO_2	Al_2O_3	
IIIA-10-a	41.10 40.75	26.32 28.25	28.14 26.12	43.01 42.84	27.53 29.70	29.43 27.46	gehlinite
IIIA-10-b	39.96	36.19	5.16	49.15	44.51	6.35	Pseudo-wollastonite
IIIA-11-a	38.07	35.18	9.56	45.97	42.48	11.54	Pseudo-wollastonite
*IIIA-11-c	33.66 30.23	31.59 27.28	4.30 5.86	48.40 47.71	45.42 43.05	6.18 9.25	Pseudo-wollastonite
IIIA-11-d	40.35 40.74	28.85 27.82	25.38 26.44	42.66 42.88	30.50 29.28	26.83 27.83	Gehlenite
IIIB-12-a	39.21 38.67	22.75 23.73	32.21 30.96	41.64 41.62	24.16 25.41	34.21 33.16	gehlenite
*IIIB-12-c	13.51	24.82	18.18	23.91	43.93	32.18	anorthite
*IIIB-12-d	16.95	22.36	16.73	30.25	40.23	29.78	anorthite
*IIIB-13-c	17.25	29.38	24.97	24.10	41.13	34.87	anorthite
*IIIB-13-e	11.68	21.16	16.31	23.76	43.06	33.19	anorthite
*IIIB-a+	30.23	25.66	23.51	38.07	32.33	29.62	gehlenite
*IIIB-a-1+	30.23	18.15	11.21	50.73	30.49	18.83	gehlenite

*precipitates small or thin

+not illustrated, but plotted on Figure 17.

TABLE C: Oxide Inclusion Composition -wt%

Inclusion	CaO = % Ca x 1.40	MnO = % Mn x 1.29	SiO_2 = %Si x 2.14	Al_2O_3 = %Al x 1.89	(CaO + MnO + SiO_2 + Al_2O_3) ≡ 100					Type
					CaO	MnO	CaO + MnO	SiO_2	Al_2O_3	
II7-b	12.94	6.53	39.55	25.95	15.23	7.69	22.92	46.55	30.54	mullite/ anorthite
*II7-d	8.99	11.92	38.35	17.80	11.67	15.47	27.14	49.77	23.10	mullite/ anorthite
*II7-f	8.05	17.19	38.46	18.92	9.74	20.81	30.55	46.55	22.90	mullite/ anorthite

* precipitates small or thin

Table D: Size Distribution of Oxides (#/cm^2)

Size Range (μm)	Steel				
	I	II	IIIA	IIIB	IV
0-5	276	110	405	261	509
5-10	138	58	144	92	338
10-15	40	15	57	64	48
15-20	24	4	4	24	9
20-25	2	2	0	7	2
25-30	0	0	0	2	4
30-35	0	0	0	0	0
35-40	0	0	0	0	0

Table E: Size Distribution of Sulfides (#/cm^2)

Size Range (μm)	Steel				
	I	II	IIIA	IIIB	IV
0-5	9623	4859	13141	27144	8096
5-10	3139	1574	4108	7913	2615
10-15	1395	760	1684	2880	1196
15-20	871	590	1092	1712	820
20-25	442	348	508	734	378
25-30	336	253	423	443	317
30-35	294	207	273	291	219
35-40	204	111	128	180	130
40-45	95	94	135	113	48
45-50	93	54	98	104	41
50-55	76	65	52	72	37
55-60	56	22	50	50	33
60-65	49	41	46	33	24
65-70	28	13	39	20	2
70-75	25	33	22	13	6
75-80	16	13	6	26	8
80-85	7	13	26	15	6
85-90	2	4	11	20	6
90-95	0	11	13	9	2
95-100	9	4	7	4	2
100-105	5	7	7	2	2
105-110	7	4	4	7	6
110-115	7	0	4	0	0
115-120	5	2	7	2	0
120-125	7	9	2	4	0
>125	9	7	15	11	4

POOR

QUALITY

ORIGINAL